Mucic Acid Loaded Polyethylenimine@Gold Nanoparticles for the Treatment of Rheumatoid Arthritis

Yixia Cui
Department of Rheumatism Immunity, Yanan University Affiliated Hospital, No.43 North Street, BaotaDistrict, Yan'an, 716000, China.

Junwei Zhang
Department of Anesthesiology, Beijing Beiya Orthopaedic Hospital, No.20 Haotian Street, Fangshan District, Beijing, 102445, China

Yanwu Liu
Department of Orthopaedic, Xijing Hospital of Air Force Medical College, No.127 Changle West Road, Beilin district, Xi'an, 710032, China

Guolin Meng
Department of Orthopaedic, Xijing Hospital of Air Force Medical College, No.127 Changle West Road, Beilin district, Xi'an, 710032, China

Changwei Lv (lucwei76@sina.com)
Department of Orthopaedic, Xi'an No.3 Hospital, The Affiliated Hospital of Northwest University Xi'an No.3 Hospital, No.10 Fengcheng 3rd Road, Xi'an, 710018, China

Research Article

Keywords: Gold nanoparticles, Arthritis, Polyethylenimine, Mucic acid, HR-TEM

Posted Date: May 20th, 2021

DOI: https://doi.org/10.21203/rs.3.rs-534531/v1

Abstract

Rheumatoid arthritis (RA) could be a common autoimmune disease that involves severe Joint deformation. The main off-target medicines unable to cure RA, that permits associate in nursing infection with the unwellness. The nanomaterials-based RA medical aid is a good strategy to enhance the treatment efficaciousness within the inflammatory region. Specifically, metal-based nanomaterials are a wonderful choice for a possible delivery vehicle for inflammatory disease agents, attributable to their novel properties. Herein, we have got developed a small-sized Polyethylenimine (PEI) coated gold nanoparticles (AuNPs) with an average diameter of 80 nm, that area unit used for top loading of carboxylic acid (MA). Various microscopic and qualitative analysis tools like high-resolution transmission microscopy (HR-TEM), Field-emission scanning microscope (FE-SEM), and Fourier-transform infrared (FTIR) spectroscopic analysis studies were accustomed to make sure as-made PEI-AuNPs. The invented PEI-coated AuNPs (PEI-AuNPs) exhibited higher contrast with an extended expanse that's promising to store giant amounts of MA medicine. MA is attributed to deduce the inflammatory response by inhibiting the pro-inflammatory cytokines and averting undesirable ancient drug aspect effects in Collagen-induced inflammatory disease (CIA). Numerous organic chemistry parameters like weight, hind paw volume, protein estimation, anti-serum protein analysis, and microscopic anatomy examination were conducted in Collagen-induced arthritis mice treated at a dose (10 μg) of MA packed PEI-AuNPs. The obtained results showed the MA-PEI-AuNPs were used with success within the treatment of Collagen-induced arthritis, relative to PEI-AuNPs and MA. Therefore, MA loaded PEI-AuNPs as a stimulating candidate in future RA applications.

1 Introduction

The impaired bone joint chronic autoimmune disorder named rheumatoid arthritis (RA) causes severe inflammation of tissue, joint degeneration, continual redness, erosive, and destruction of the bone tissue [1]. Completely different types of a substance cause severe bone destruction of RA, antibodies, and secretion of various styles of pro-inflammatory cytokine/chemokine like lymphokine (IL)-6, IL-1β, IL-17 and Interferons (IFN), prostaglandin E2, metalloproteinases (MMPs), and tumor necrosis factor (TNF-α) [2, 3]. The secretion of the pro-inflammatory cytokines is answerable for activating the massive proportion of invasive macrophages to hurry up and triggers RA progression via regulation of inflammation micro-environment [4]. Therefore, the RA treatment appears to be entirely dependent on suppressing the inflammatory reaction. Still, there's no impact of medication on the RA treatment, because of its expansive cost, long facet effects, and off-target medication [5]. Additionally, various medication types like biological agents, anti-rheumatic medication, immuno-suppressant steroid hormones, and anti-inflammatory medication are offered to use as therapeutic agents to deduce inflammatory and Joint severity in RA [6, 7]. Therefore, the necessity to fabricate anti-arthritis agents can have fewer facet effects, cheap and longer life, that have the flexibility of transforming bone joint defects, suppress the secretion of the pro-inflammatory protein, and severe inflammation. Plant-based secondary metabolites like flavonoids are well-known and most effective therapeutic agents obtained from varied

fruits, leaves, roots, etc. It exhibits medicine, immunomodulatory, and inhibitor properties [8, 9]. Earlier reports powerfully discerned the naturally earned flavonoids will deduce the inflammatory response and transform bone defects in a short period [10].

Mucic acid (MA) or a pair of, 3,4,5-Tetrahydroxyhexanedioic acid may be a phytocompound obtained from *Phyllanthus Emblica*. MA and its derivatives are found to possess antimicrobial, anti-diabetic, and anti-inflammatory properties. To our information, the osteogenic potential of MA has not been reported yet. An oversized fraction of phytocompounds is water-insoluble and crystalline, thereby proscribing their direct application within the flesh. This necessitates the necessity for material-based delivery of phytocompounds to the wound site since it ensures higher bioavailability. The metal nanoparticle-based carboxylic acid delivery can greatly impact RA treatment [14, 15]. Attributable to the ability to scavenge free radicals and lack of harmful, gold nanoparticles (AuNPs) are extensively used nanomaterials in various applications and RA medical aid [16]. On the opposite hand, the designer is among the foremost extensively used polycations in drug delivery, because of its high transfection potency [17, 18]. It is coating on the AuNPs exterior provides most stable in biological fluid and had all-time low toxicity then clean AuNPs [19]. Therefore, the PEI coated AuNPs as a unique framework to treat RA. This investigation's key purpose regarding the bone restorative effects and deduce the pro-inflammatory protein by delivering MA by PEI-AuNPs and exploring its accented regulative mechanisms on in vivo collagen-induced inflammatory disease (CIA) mice model.

Herein, this study focuses on developing an artificial route accomplished through using HAuCl4 for manufacturing AuNPs. The PEI was then inserted into the AuNPs (PEI-AuNPs) surface, which is accustomed to comprehend vital quantities of carboxylic acid (MA). The AuNPs and PEI-AuNPs developed were generally confirmed by TEM, FE-TEM, and FTIR. The MA encapsulated PEI-AuNPs are then accustomed to boost the treatment of RA with more effectiveness. The biochemical results have steered creating the processed MA-PEI-AuNPs a promising candidate for CIA therapy.

2 Materials And Methods

2.1 Materials

Gold(III) chloride hydrate ($HAuCl_4$) (99.9%), MAphinidin chloride ($C_{15}H_{11}ClO_7$), Trisodium citrate ($Na_3C_6H_5O_7$), polyethylenimine (PEI, *Mw*2,500) and 70% ethanol, Dulbecco's modified eagle medium (DMEM), fetal bovine serum (FBS), penicillin and streptomycin (PS) were purchased from Shanghai, China.

2.2 Synthesis of PEI coated AuNPs

To fabricate PEI-coated AuNPs, 0.02% $HAuCl_4$ solution (200 mL) and 1.5 mL of 1% (w/w) PEI solution were added into the beaker containing 50 mL of distilled water (dH_2O) and then vortexed at room temperature for 24 h. Afterward, PEI-coated AuNPs were collected by centrifugation at 10,000 rpm for 15

min and washed twice with dH_2O and ethanol. The PEI-coated AuNPs solution was kept at 4 ˚C to avoid aggregation.

2.3 Nanomaterial Characterization

Studies of electron microscopy were used to evaluate the PEI-AuNPs structure, size, and composition. Transmission electron microscopy (TEM, JEOL JEM-2100) images of the material were taken using HR-TEM at a wavelength of excitation of 200 kV. The solution PEI-AuNP was mounted on a 200-mesh copper grid and was vacuum-dried at 37 ° C using a hot air oven. After complete dried, the PEI-AuNP was pictured at 100 kV. The PEI-AuNP was examined using Field Emission Scanning Electron Microscope (FESEM, 5 kV permitted Quanta 200 FEG to operate) to examine the scale, shape and structure of the produced NPs. In studying the surface charge and size of PEI-AuNPs, a zeta sizer (Nano-ZS, Malvern Instruments) was used. For FTIR experiments, the powder form of PEI-AuNPs was combined with KBr powder and converted into pellets. The spectrum was obtained in transmission mode using Fourier transform infrared (FTIR, Nicolet 6700 (Thermo Fisher, USA) spectrometer with a measurement range of 4000 – 400 cm^{-1}.

2.4 Mucic acid entrapment efficiency

Evaluation of MA drug moiety trap efficacy on the surface of PEI-AuNPs was calculated by UV-Visible spectrometry by measuring the absorption spectrum of collected post-centrifugation supernatant after stirring the NPs with MA. The absorbances of MA released from the scaffolds were measured at 190 nm, and the concentration of MA was deduced using its standard graph. Then, the effectiveness of the trapping was calculated using the formula given below:

$$\% \text{ Entrapment Efficiency} = [(T_{MA} - F_{MA})/T_{MA}] \times 100$$

Where T_{MA} is measured as the total value of introduced MA and F_{MA} is the sum of free MA in the supernatant [20].

2.5 Animals

Eight weeks of old male albino rats with 180–210 g of albino strain were acquired and kept inside a hygienic animal house maintained at 25 ± 3°C condition, and providing proper, limitless access to water and standard pellet diet, except in conduct experiments. The animal committee of the National Institutes of Health Guide for Care and Use of Laboratory approved 7 days prior to the initiation of the study and its guidelines used during animal experiment protocols.

2.6 Collagen-Induced Arthritis in Wistar Rats

Bovine type II collagen (CII) formulated by using well-defined protocol and prepared CII has been dissolved at 2 mg / mL in 0.05 M acetic acid by slowly vortexed overnight at 4 ° C. Then, CIA was arousing 16 albino male rats using the footpad method. Each male rat was subcutaneously immunized in an unfinished Freund's adjuvant (IFA) emulsifying agent with 0.2 mg CII per rat into the left hind paw at day 0. Immunized male rats were divided into four treatment group (N = 4): I control group (without CIA

induction), (ii) PEI-AuNP group, (iii) MA-PEI-AuNP-treated CIA group. Protective therapy took place from day 0 till day 7. Then, the daily intra-articularly (i.a) injection (except weekends) into ankle joints with different forms of NPs. The treatment was initiate for 7 consecutive days [21].

2.7 Measurement of Body weight and Organ Weight of Rats with CIA

The male albino rats were weighed using digital balance after finishing the 7, 14, 21, and 28 days of treatment. The final and initial body volume was taken for each control group and treated rat group. At the end of the tests, the mice were exposed to anaesthetic with xylazine and ketamine. Following the treatments, the major internal organs like liver, spleen and thymus and blood were obtained for rapid measurement and stored for more assessment at − 80 ° C.

2.8 Histological Examination of Rats with CIA

After the Euthanasia performed, each animal's right knee joints have been collected and fixed overnight with PBS (pH 7.4) in a 4 percent formalin buffer. After the decalcification of extracted knee joints in 10 percent nitric acid (HNO_3). Every animal's joint tissue parts were deposited in paraffin which was cut utilizing microtome device to 4 μm parts. Then, for histological observation under a 400 x magnifying microscope, the acquired sliced tissue segment stained with hematoxylin-eosine (H&E). Histological examination of internal sections into joint tissues including such soft periarticular tissues, cartilage and synovial membrane is observed and distinguish the markedly different features between the control and MA-PEI-AuNPs was evaluated [22].

2.9 Measurement of biochemical parameters

Blood samples were taken from albino male rats treated with MA-PEI-AuNPs for rapid quantification of serum pro-inflammatory cytokines, includeIL-6, TNF-α, IL-1β and PGE2 utilizing standard experimental procedures following the completion of the experimental duration (28 day). Then, the serum anti-CII IgG antibody was also evaluated using a rat serum anti-CII antibody ELISA kit.

2.10 Statistical Analysis

All the results are expressed as mean ± standard error mean (SEM) (n = 4). Two-way variance analysis (ANOVA) was used to calculate volume of the hind paw and analyze the biochemical parameters. Statistical significance as presented in the tables and figures was expected at $p < 0.05$ and $p < 0.01$.

3 Result And Discussion

Herein, we have designing well-established mucic acid (MA) packed PEI-AuNP nanomaterial using a blend of AuNPs and PEI, which are the most noteworthy materials for treating Collagen-Induced arthritis (CIA).

3.1 Morphological Analysis

As depicted in Fig. 1A, the FE-SEM image shows the AuNPs metal oxide nanostructure. The result suggests that the as-prepared AuNPs well-dispersed small-sized with spherical shape. Figure 1A denotes HR-TEM images showing that the AuNPs were surrounded by the thinner PEI coated layer (grey). The high-contrast metal nanostructure and low-contrast coating were observed. The average diameter of AuNPs was estimated from the HR-TEM image to be 182.5 ± 10 nm. The nanomaterials with tiny sizes ranging from 1–200 nm gathered are associated with the upper hand of nanoparticles in drug delivery applications in terms of improved bioavailability, increased discharging of drugs, high cell absorption, and increased surface-area-to-volume ratio, actuating more space for cellular interactions [23].

3.2 DLS and FTIR Analysis

The corresponding DLS study is shown in Fig. 2A; the approximate size distribution of the AuNPs was 198.5 ± 5 nm. The surface charge of the as-synthesized AuNPs and PEI coated AuNPs were determined by Zeta potential analyzer. It was determined to be + 26.6 mV in AuNPs, and the noted zeta potential was + 34.4 mV due to the presence of PEI coating on the surface of Au NPs, as shown in Fig. 1B. The obtained zeta potential values displayed plausible stability [25]. FT-IR spectroscopy was demonstrated after AuNPs manufacturing (Fig. 1C) to attest to functional groups' existence in the AuNPs. The peaks at 2918 and 2855 cm^{-1} bands correspond to the C-H bond formation which confirms AuNPs formation. The characteristic band at 3425 cm^{-1} was due to –OH group in the MA [26]. It showed characteristic 2925 and 1630 cm^{-1} bands indicating methyl group and amide I for bonding C-O. Broadband at 3430 cm^{-1} corresponding to the N-H stretch vibration of PEI.

3.3 Drug Releasing Study

The encapsulating hydrophobic nature of MA onto the surface of AuNPs and PEI-AuNPs is based on the hydrophobic or electrostatic interactions. The MA loading content of PEI-AuNPs (mass of MA in the PEI-AuNPs /mass of PEI-AuNPs loaded with MA×100%) and loading efficiency (mass of MA attained in the PEI-AuNPs /mass of the feeding MA×100) 0.012/0.014×100 = 85.7% of MA in PEI-AuNPs was calculated to be 18.8 wt%. As depicted in Fig. 3, the in vitro MA discharge profile from PEI-AuNPs was determined by the dialysis bag analysis at different pH viz pH 7.4 and pH 6.8 at 37°C. It shows the release of MA from PEI-AuNPs the release rates of flavonoid in solutions of pH 7.4 and pH 6.8 in 24 days were 65% and 74%, respectively. On the contrary, the gradual degradation of PEI on the surface of the AuNPs depends upon acidic nature; it improves the loading and sustainable release of MA from PEI-AuNPs. Adding PEI prevents the burst release of MA from PEI-AuNPs as its carbonyl groups associated with the amine and hydroxyl groups, ensuring gradual surface erosion [27].

3.4 Behavioral Test

The bodyweight of the different nano-formulation treated mice groups was evaluated shown in Fig. 4A, showing no difference in the body weight between the control and MA-PEI-AuNPs treated mice group, except these the rats treated with AuNPs and CIA groups (without any treatment) after the 28 days, which

shown significantly decreased body weight observed. Because of the severity of the CIA, a significant loss of body weight in CIA groups (without any treatment) and no significant effect on the CIA in AuNPs group is seen. In addition, due to its strong anti-inflammatory and antioxidant effects of MA, the incidence of CIA was significantly deduced while being treated with MA-PEI-AuNP, as a result of which the severity of body weight deduction was recovered. No major abnormalities were found in the volume of the hind paw in the joints of the healthy rats (control group) in Fig. 4B. Twenty-four days later, the hind paw was noticed its maximum severity in the CIA induction group (saline-treated) due to CIA severity influencing a significant hind paw swelling as a result of critical inflammation allowing disease to reach its maximum severity and no significant effect on joint swelling was observed in the AuNPs treated group. In addition, MA-PEI-AuNPs treated group, suppressed joint swelling up to the day 24 days which show an anti-inflammatory effect, as a result, the inflammation was gradually resolved.

Figure 5 indicates the relative weight of internal organs of four studied groups of rats. At the end of the experimental duration, the rat groups caused by the GIA had significantly increased organ weight relative to control and MA-PEI-AuNPs ($P < 0.01$). There was no difference in the absolute weight of the spleen, thymus, and liver between the MA-PEI-AuNPs treated and the control group respectively. The positive effect of MA-PEI-AuNPs non-toxic nature on spleen, thymus, and liver was observed in rat MA related to healthy rat. A remarkable impact has been found in the MA-PEI-AuNPs community on the internal organs due to their beneficial anti-arthritis effects caused by the combination of MA medication and AuNP. In the case of CIA-induced rats (saline-treated) and AuNPs, an index of undesirable side effect was observed, as result gradual decrease in the weight of the internal organ after the treatment.

3.5 Histological Examination of Rats with CIA

According to H&E staining results (Fig. 6A), when compared to MA-PEI-AuNPs, the ankle joint region of the rat with arthritis displays some dashed red or ellipses-shaped structure denoted as a large area of inflammation. Since it possesses strong metabolism, the CIA-induced rat MA show deduced blue staining. By comparison, the rat community induced by the CIA treated with groups of MA-PEI-AuNPs shows much larger blue areas, which means that the antioxidant capacity of MA-PEI-AuNPs could effectively penetrate the inflammatory region and can maintain it better in the inflammatory region [28]. The group treated with MA-PEI-AuNPs did not show degradation of the bone and erosion with joint space was found to be quite small. Hence, the H&E staining observation findings showed that ameliorated bone degeneration in the ankle joint was influenced by subcutaneous administered core-shell MA-PEI-AuNPs (Fig. 6C).

3.6 Measurement of biochemical parameter

Figure 7 and 8 showed the expression profile of pro-inflammatory factors such as the expression interleukin (IL)-1β, IL-6, IL-17, and PGE2. Arthritis pathogenesis had an important part to play in the acceleration. Various types of antigen, antibody, and pro-inflammatory cytokine such as interleukin (IL)-1β, IL-6, interferon (IFN), prostaglandin E2 (PGE2), metalloproteinases (MMPs), and tumor necrosis

factor (TNF-α) are mainly accomplished to participate in the earliest RA systemic autoimmunity growth incident [29, 30]. Secreting different pro-inflammatory cytokine is responsible for activating a large number of infiltrating macrophages to speed up and induce RA development through inflammatory microenvironment regulation. Hence, RA's approach to the treatment is primarily dependent on inhibiting the inflammatory response. Furthermore, IL-17 was triggered by IL-6 that is a central cytokine in RA pathogenesis and contributes to both joint damage and extra-articular signs. The high levels of IL-6 and IL-17 have thus grown in the plasma and synovial fluid of the CIA model, and are participating in the development of RA. IL-17 is usually predominantly generated by T-helper 17 cells (Th17 cells), and IL-6 [31, 32] causes the differentiation of naive T cells into Th17 cells. The elevated pro-inflammatory rates are largely responsible for the severity of induced arthritis. The serum from joint tissue was obtained in the current study after the 28-day treatment of the distinct saline and nano-drug formulations; the increasing incidence of pro-inflammatory factors such as IL-1β, IL-6 & IL-7, and PGE2 was noted in the CIA-induced rat group.

In the case of the MA-PEI-AuNPs treated rat group, significant cytokine rates greatly decreased to the CIA-induced rats. The quantification of serum anti-CII antibody was noted in control in Fig. 8A, CIA-induce rat group, AuNPs and treated group MA-PEI-AuNPs using ELISA kit. Additionally, severe inflammation and knee joint damage group influence serum anti-CII antibody CIA induce rat as a result of framework encourages anti-CII antibody production rate. In the case of treated rats with MA-PEI-AuNPs, the deduced serum anti-CII antibody rate was observed because of its anti-inflammatory effect. B-lymphocytes are primarily capable of generating collagen-specific antibodies that can develop immune complexes with different antigens and associate easily with complementary elements to start inflammation in the joint tissue. Previous research suggested a possible association between auto-antibody responses and restorative effects which correlates clinical symptom improvement with auto-antibody degree of suppression [33, 34].

4 Conclusions

To conclude, AuNPs coated with PEI to generate PEI-AuNPs, we have designed new synthetic method to create AuNPs that is excellently established. Instead, the PEI-coated AuNPs nanostructure was encapsulated by electrostatic attraction with mucic acid (MA). PEI-coated AuNPs are notable materials for the treatment of arthritis. The present study demonstrated that the impacts of saline, AuNPs and MA loaded PEI-AuNPs were subjected to CIA therapy assessment. Among them, flavonoid loaded PEI-AuNPs recognized the powerful anti-arthritis agent to deduce CIA in rats as compared to others. In which MA-PEI-AuNPs reduced significantly the pro-inflammatory component, and mentioned the new bone growth. In the CIA-induced rat group, because of the maximum severity of the inflammation, the increased risk of the arthritis index was found to be more important, and AuNPs have a slightly anti-inflammatory activity. Hence, MA-PEI-AuNPs may represent as an appropriate anti-arthritis in the potential development of arthritis. Finally, it severely suppressed the formed swelling, erythema, and ankylosis of the hind paw and ankle joints due to their antioxidant and anti-inflammatory features.

Declarations

Acknowledgement

This research was supported by a grant from the Key Research and Development Program of Shaanxi Province (No. 2019-SF-194).

References

1. Y. Ma, Y. Song, F. Ma, G. Chen, Journal of Inorganic and Organometallic Polymers and Materials. 1–10 (2019)
2. P.D. Harvey, J. Plé, Journal of Inorganic and Organometallic Polymers and Materials, 1–42 (2021)
3. B. Han, D. Peng, J. Wang, Z.N. Lu, J. Inorg. Organomet. Polym Mater. **31**, 22–31 (2021)
4. S.F. El-Amin, M.S. Kwon, T. Starnes, H.R. Allcock, C.T. Laurencin, J. Inorg. Organomet. Polym Mater. **16**, 387–396 (2006)
5. L.D. Quan, G.M. Thiele, J. Tian, D. Wang, Expert Opinion on Therapeutic Patents. **18**, 723–738 (2008)
6. P. Li, Y. Zheng, X. Chen, Front. Pharmacol. **8**, 460 (2017)
7. T.D. Wilsdon, C.L. Hill, Australian prescriber. 40, p.51 (2017)
8. A.N. Panche, A.D. Diwan, S.R. Chandra, Journal of nutritional science. 5 (2016)
9. A.M. Abdel-Azeem, S.M. Zaki, W.F. Khalil, N.A. Makhlouf, L.M. Farghaly, Frontiers in Microbiology. **7**, 1477 (2016)
10. M.H. Pan, C.S. Lai, C.T. Ho, Food & function **1**(1), 15–31 (2010)
11. T.C. Wallace, M.M. Giusti, Advances in Nutrition. **6**, 620–622 (2015)
12. H.E. Khoo, A. Azlan, S.T. Tang, S.M. Lim, Food & nutrition research **61**, 1361779 (2017)
13. M.H. Jeong, H. Ko, H. Jeon, G.J. Sung, S.Y. Park, W.J. Jun, Y.H. Lee, J. Lee, S.W. Lee, H.G. Yoon, K.C. Choi, Oncotarget. **7**(35), 56767 (2016)
14. C.T. Pham,. Wiley Interdisciplinary Reviews: Nanomedicine and Nanobiotechnology. 3, 607–619 (2011)
15. A. Mani, C. Vasanthi, V. Gopal, D. Chellathai, Int. Immunopharmacol. **41**, 17–23 (2016)
16. H. Nah, D. Lee, M. Heo, J.S. Lee, S.J. Lee, D.N. Heo, J. Seong, H.N. Lim, Y.H. Lee, H.J. Moon, Y.S. Hwang, Science and technology of advanced materials. **20**, 826–836 (2019)
17. A. Mani, C. Vasanthi, V. Gopal, D. Chellathai, Int. Immunopharmacol. **41**, 17–23 (2016)
18. S. Taranejoo, J. Liu, P.K. Verma, Hourigan, Journal of Applied Polymer Science. 132 (2015)
19. C. Hu, Q. Peng, F. Chen, Z. Zhong, R. Zhuo, Bioconjugate chemistry **21**, 836–843 (2010)
20. C. Murugan, M. Rajkumar, N. Kanipandian, R. Thangaraj, K. Vimala, S. Kannan, Curr. Sci. **118**, 1583 (2020)

21. M.M. Ansari, A. Ahmad, R.K. Mishra, S.S. Raza, R. Khan, ACS Biomaterials Science & Engineering. **5**, 3380–3397 (2019)
22. C.Y. Tsai, A.L. Shiau, S.Y. Chen, Y.H. Chen, P.C. Cheng, M.Y. Chang, D.H. Chen, C.H. Chou, C.R. Wang, C.L. Wu, Arthritis & Rheumatism: Official Journal of the American College of Rheumatology. 56, 544–554 (2007)
23. R. Singh, J.W. Lillard Jr., Nanoparticle-based targeted drug delivery. Experimental and molecular pathology. **86**, 215–223 (2009)
24. H. Singh, J. Du, P. Singh, T.H. Yi, Artificial cells, nanomedicine, and biotechnology. 46,1163–1170 (2018)
25. D. Jain, R. Banerjee, J. Biomed, Mater. Res., Part B. **86**, 105–112 (2008)
26. A.S. Abd Raboh, M.S. El-khooly, M.Y. Hassaan, Journal of Inorganic and Organometallic Polymers and Materials, 1–12 (2021)
27. P.C. Pandey, G. Pandey, R.J. Narayan, Biointerphases. **12**, 011005 (2017)
28. S. Tummala, M.S. Kumar, S.K. Pindiprolu, Improved anti-tumor activity of oxaliplatin by encapsulating in anti-DR5 targeted gold nanoparticles. Drug Deliv. **23**(9), 3505–3519 (2016)
29. S. Ueha, F.H. Shand, K. Matsushima, Frontiers in immunology **3**, 71 (2012)
30. R. Domingo-Gonzalez, O. Prince, A. Cooper, S.A. Khader, Tuberculosis and the Tubercle Bacillus. 33–72 (2017)
31. C. Yang, Z. Daoping, X. Xiaoping, L. Jing, Z. Chenglong, J. Microencapsul. **37**, 77–90 (2019)
32. M. Komiyama, T. Mori, K. Ariga, Bull. Chem. Soc. Jpn **91**, 1075–1111 (2018)
33. S.D. Vita, F. Zaja, S. Sacco, A.D. Candia, R. Fanin, G. Ferraccioli, Arthr. Rhuem. **46**, 2029–2033 (2002)
34. B. Marston, A. Palanichamy, J.H. Anolik, Current opinion in rheumatology. **22**, 307 (2010)

Figures

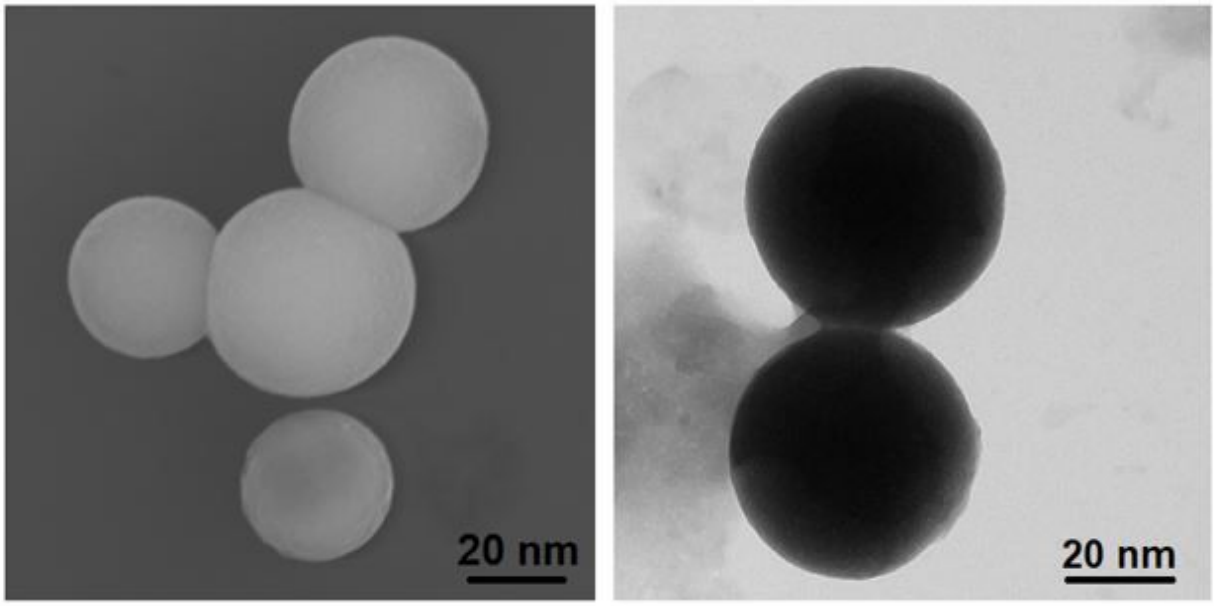

Figure 1

Physical and chemical characterization of PEI coated AuNPs. (A) FE-SEM and (B) HR- TEM image of PEI-AuNPs clearly showing the small sized spherical shaped nanostructure.

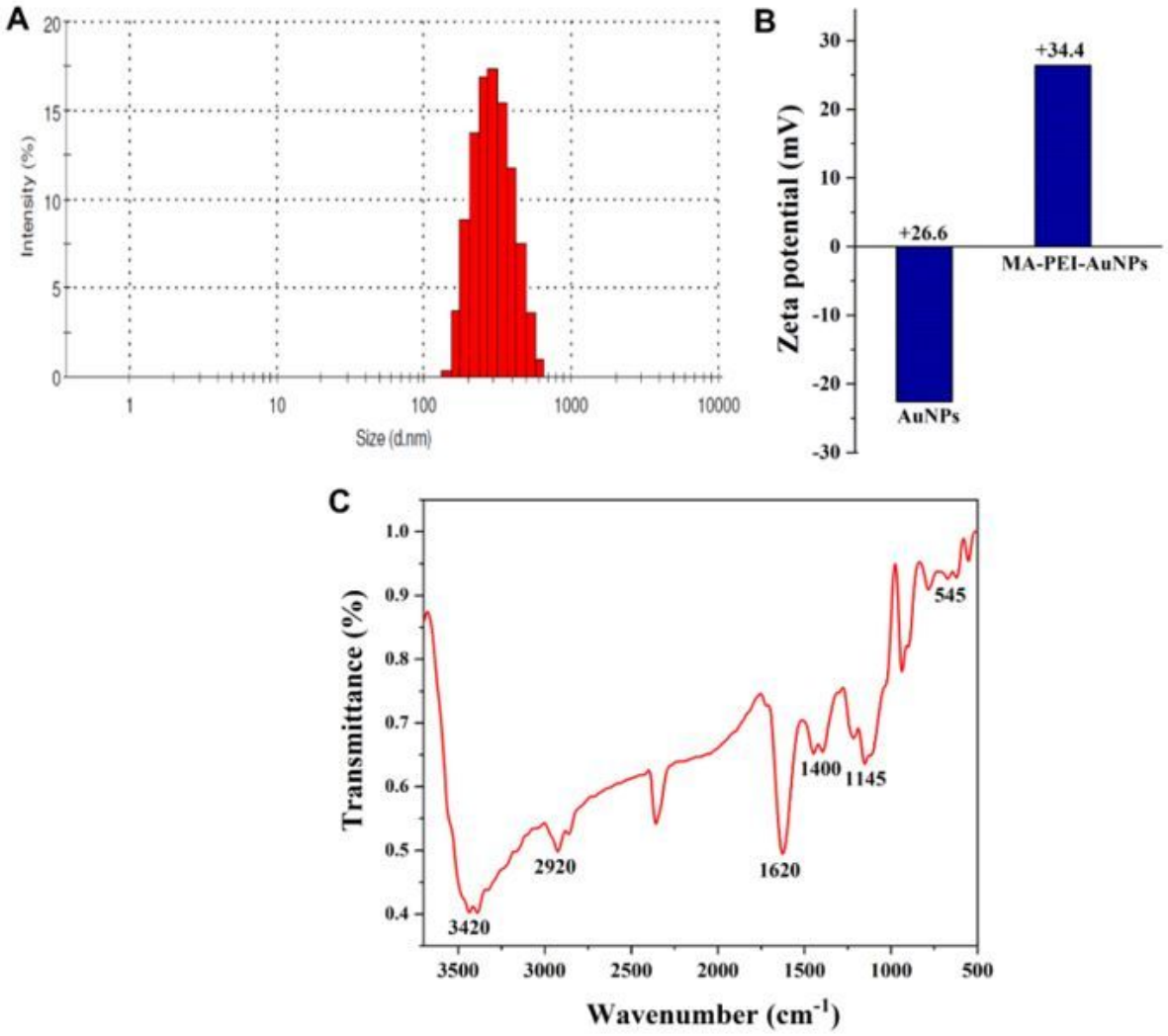

Figure 2

(A) DLS studies on size distribution, (B) zeta potential and (C) FT-IR spectrum of the PEI-AuNPs.

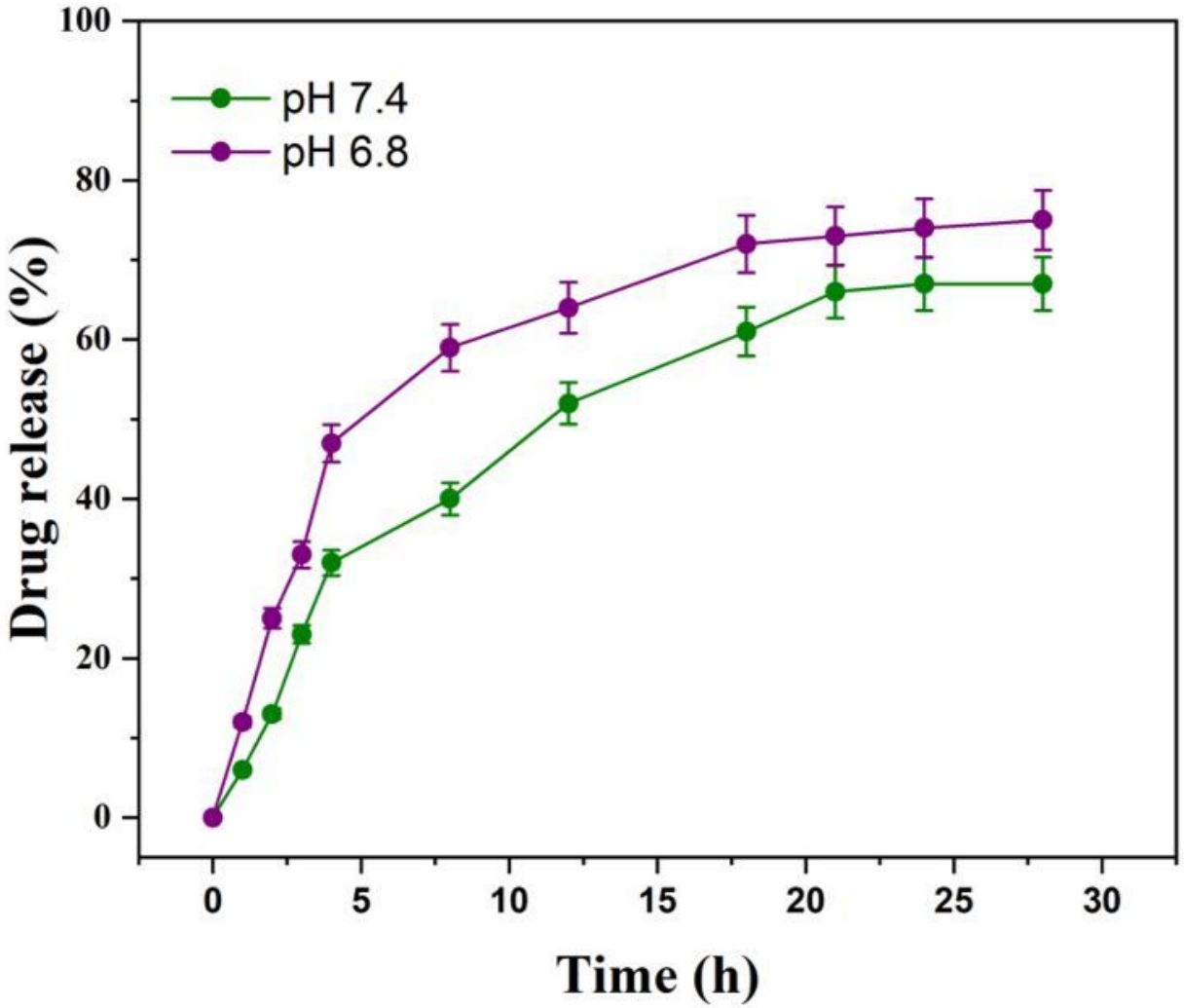

Figure 3

Drug discharging profile of nanoparticles.MA release profile from PEI-AuNPs was demonstrated under pH 7.4 and pH 6.8 at 37 °C for 28 days

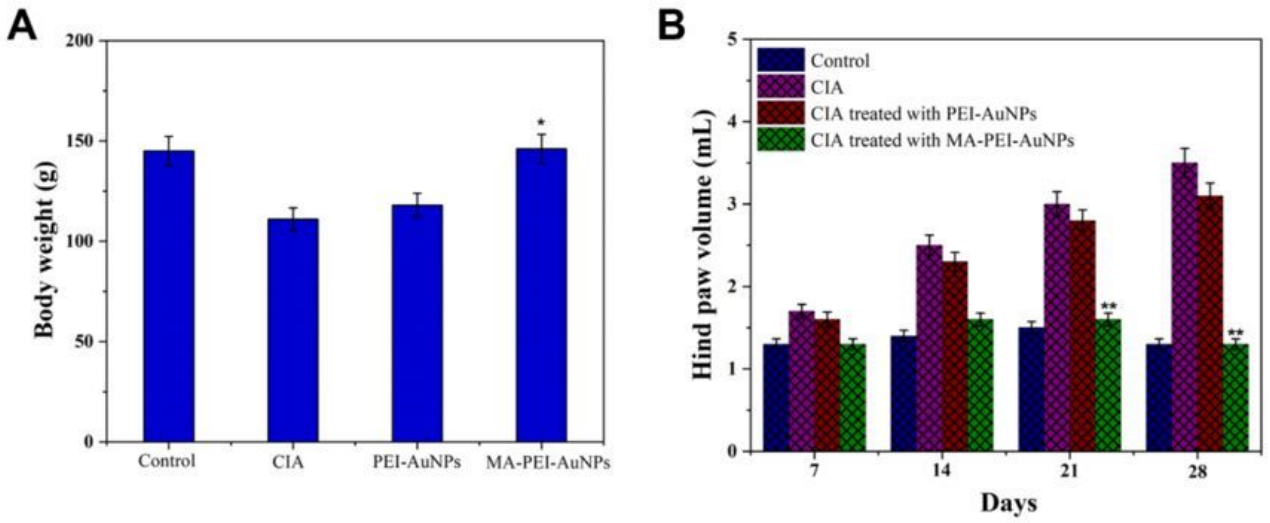

Figure 4

(A) body weightof different group of mice such as control (normal mice with saline treated), CIA induced mice without treatment, CIA induced mice treated with PEI- AuNPs and CIA induced mice treated with MA-PEI-AuNP after the treatment time (28 days) and (B) Hind paw volume for four different mice group are considered as a set displayed after the treatment. Four different mice in a set consists a control (Normal mice with saline treated), CIA induced mice (without any treatment), CIA induced mice treated with PEI-AuNPs and CIA induced mice treated with MA-PEI-AuNPat different time intervals (7, 14, 21 and 28 days).

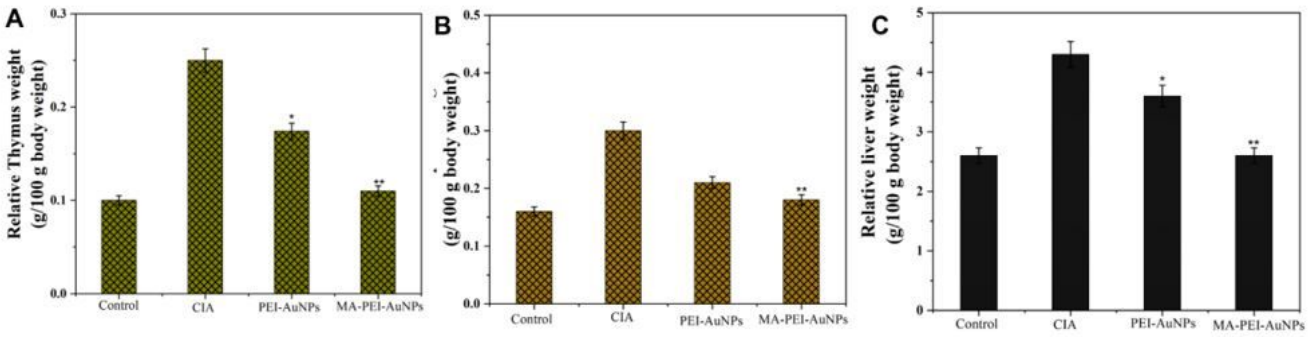

Figure 5

(A) Spleen (B) Thymus and (C) liver weight of four different rat groups after the treatment (Control, CIA induced rat, CIA induced rat treated with AuNPs, and CIA induced rat treated with MA-PEI-AuNPs (n=4).

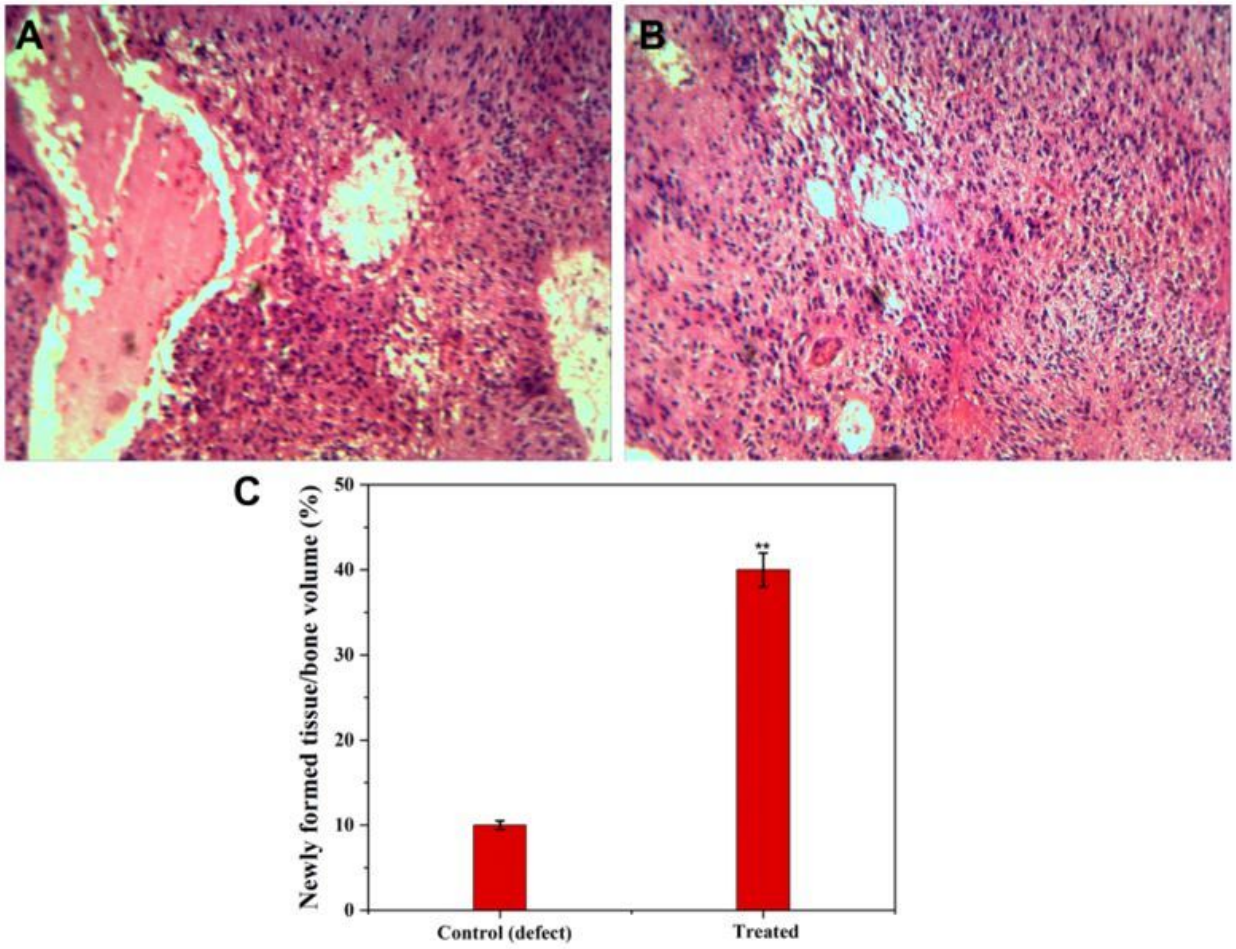

Figure 6

Histological analysis of (A) CIA induced ratgroup and (B) MA-PEI-AuNPstreated rat group(5 mg/mL) by treated rats were examined by hematoxylin and eosin (H&E) staining of the ankle joint. The damaged regions including, synovial inflammation and bone destruction and(C) total volume of new bone tissue formation after 28 days (40xMagnification).

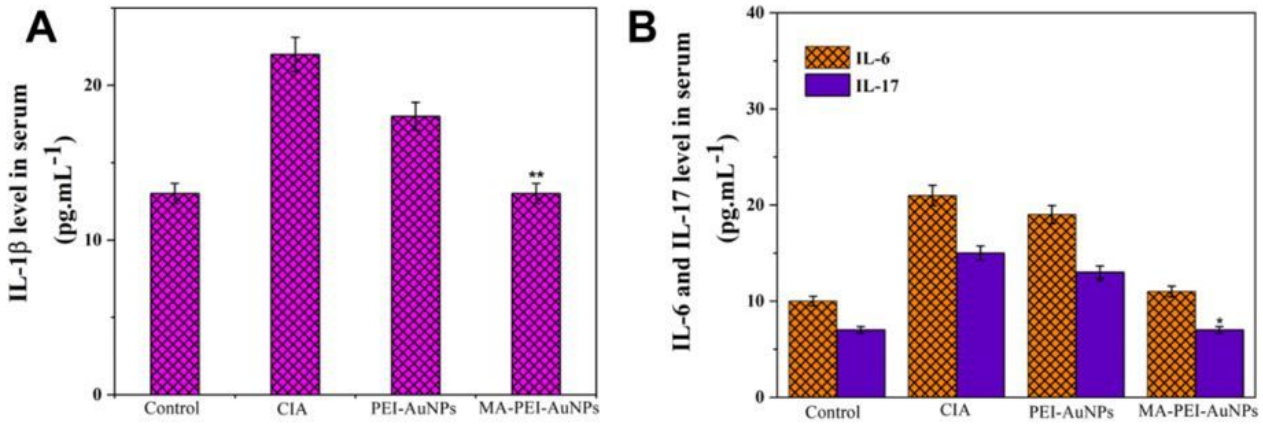

Figure 7

(A) IL-1β and (B) IL-6 & IL-7 expression profile was assessed by ELISA after the treatment with the four different groups for 28 days (n=4).

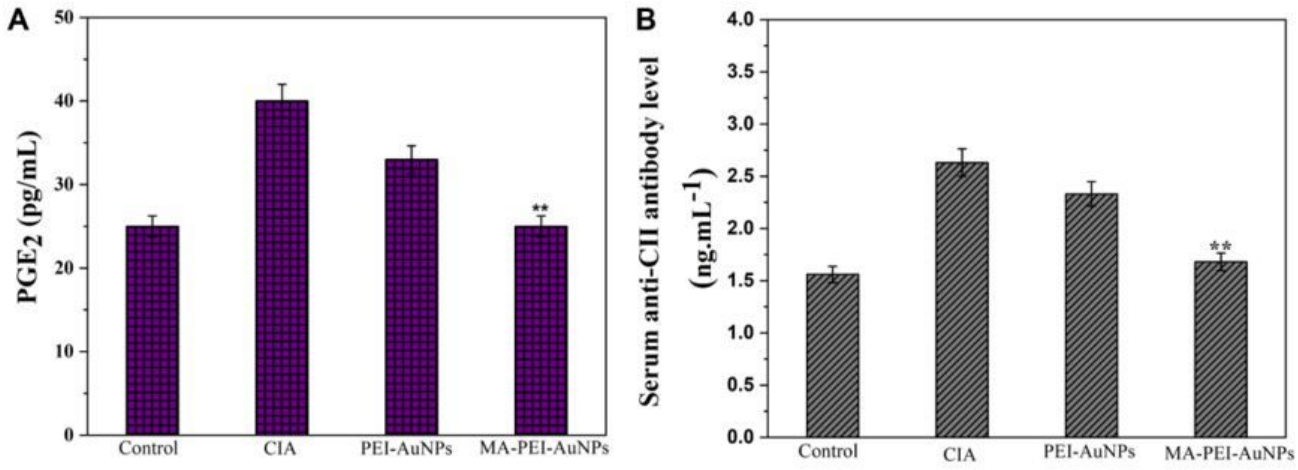

Figure 8

(A) PGE2 and (B) Serum anti-CII antibody expression profile was assessed by ELISA after the treatment with the four different groups for 28 days (n=4).